

# Dynamic NOMA-Based Computation Offloading in Vehicular Platoons

Dongsheng Zheng, Yingyang Chen, *Member, IEEE*, Lai Wei, Bingli Jiao, *Senior Member, IEEE*, and Lajos Hanzo, *Fellow, IEEE*

**Abstract**—Both the Mobile edge computing (MEC)-based and fog computing (FC)-aided Internet of Vehicles (IoV) constitute promising paradigms of meeting the demands of low-latency pervasive computing. To this end, we construct a dynamic NOMA-based computation offloading scheme for vehicular platoons on highways, where the vehicles can offload their computing tasks to other platoon members. To cope with the rapidly fluctuating channel quality, we divide the timeline into successive time slots according to the channel's coherence time. Robust computing and offloading decisions are made for each time slot after taking the channel estimation errors into account. Considering a certain time slot, we first analytically characterize both the locally computed source data and the offloaded source data as well as the energy consumption of every vehicle in the platoons. We then formulate the problem of minimizing the long-term energy consumption by optimizing the allocation of both the communication and computing resources. To solve the problem formulated, we design an online algorithm based on the classic Lyapunov optimization method and block successive upper bound minimization (BSUM) method. Finally, the numerical simulation results characterize the performance of our algorithm and demonstrate its advantages both over the local computing scheme and the orthogonal multiple access (OMA)-based offloading scheme.

**Index Terms**—Computation offloading, non-orthogonal multiple access (NOMA), vehicular platoons, Lyapunov optimization, block successive upper bound minimization (BSUM).

## I. INTRODUCTION

THE Internet of Vehicles (IoV) has attracted substantial attention both in industry and academia with the objective of improving traffic efficiency and improving road safety [1]–[4], by sharing information among vehicles and roadside units (RSUs) within their coverage area. Typical applications include safety-related, driving-assistance and passenger entertainment services [5]. The safety-critical tasks are mainly executed locally by the on-board unit for eliminating any queuing and communications delays as well as transmission impairments. By contrast, entertainment services readily tolerate some delay. In a nutshell, the demands for computing resources have increased quite dramatically owing to the augmented security requirements and expectations of passengers, especially when aiming for taking into account the

environmental awareness of all other vehicles in their decision-making.

To overcome these challenges, mobile edge computing (MEC) and fog computing (FC) constitute a pair of promising design paradigms for offloading computing-intensive tasks to the edge of the mobile networks and fog nodes [6]–[9]. As a benefit of closer proximity to computing servers, the data transmission delay can be significantly reduced in MEC-aided or FC-assisted vehicular networks, which substantially improves their efficiency. In urban scenarios, the computing nodes are usually part of the roadside units (RSUs) [10], [11]. However, it is costly to deploy lots of RSUs along all highways. As a design alternative, we consider vehicular platoons, which exhibit slowly varying formations [12], [13], where vehicles may offload their tasks to their platoon members having fewer or less demanding computing tasks. This also supports the option of formulating decisions based on the joint environmental awareness of the nodes in the platoon, taking into account the sensory information of all vehicles in it.

In vehicular communications, spectrum shortage is another issue when considering data transmission among vehicles requesting computation offloading and those assisting in offloaded processing. In this context, non-orthogonal multiple access (NOMA) can serve several users within the same time and frequency resource block, which further improves the bandwidth efficiency [14], as evidenced in [15]–[18].

Motivated by the above-mentioned aspects, we construct a NOMA-based computation offloading scheme for infotainment applications. Specifically, the vehicles in the platoon can offload computing tasks to the neighboring vehicles or retrieve results from other platoon members having less computing tasks by relying on the dedicated short-range communications (DSRC) protocol or on the cellular-vehicle-to-everything (C-V2X) protocol [19]. Given the potentially high speed of vehicles we assume having an uncorrelated Rayleigh fading channel model and conceive an online algorithm for making offloading decisions for allocating the communication resources according to the near-instantaneous channel conditions and additionally taking into account the task queues of the vehicles in each time slot. The channel estimation errors are also taken into account in the vehicular platoons.

The main contributions of our paper are summarized as follows:

- We propose a dynamic NOMA-based computation offloading scheme for a vehicular platoon. The problem of minimizing the long-term energy consumption of the whole platoon is formulated for optimizing the offloading

D. Zheng, L. Wei, and B. Jiao are with the Department of Electronics, Peking University, Beijing 100871, China (e-mail: zhengds@pku.edu.cn; future1997@pku.edu.cn; jiaobl@pku.edu.cn).

Y. Chen is with the College of Information Science and Technology, Jinan University, Guangzhou 510632, China (e-mail: chenyy@jnu.edu.cn).

L. Hanzo is with the School of Electronics and Computer Science, University of Southampton, Southampton, SO17 1BJ, U.K. (email: lh@ecs.soton.ac.uk).

decisions and the communication resource allocation.

- We design the computing and offloading decisions on a time-slot by time-slot basis and take the channel estimation errors into account.
- In order to solve the problem formulated, we propose an online algorithm based on the classic Lyapunov optimization method [20] and on the block successive upper bound minimization (BSUM) method [21].
- Finally, the advantages of NOMA-based computation offloading over both local computing and orthogonal multiple access (OMA)-based offloading are quantified.

The remainder of this paper is organized as follows. We discuss the related literature in Section II. Then, we introduce our system model and formulate the optimization problem considered in Section III. The algorithm scheduling the computation offloading and resource allocation decisions is designed in Section IV. Finally, our simulation results are given in Section V, and Section VI concludes this paper.

## II. RELATED CONTRIBUTIONS

NOMA-based computation offloading has been shown to enhance the performance of MEC and FC systems [22]–[32]. The existing studies can be divided into two categories according to whether static or dynamic NOMA-based computation offloading is considered in the problem formulation.

For *static NOMA-based computation offloading*, diverse optimization metrics have been investigated. To minimize the energy consumption, the authors of [22] considered a scenario where both the task offloading and result retrieval relied on NOMA. Moreover, the authors of [23] studied NOMA-based computation offloading among mobile devices, where beamforming was introduced for reducing the interference among different NOMA pairs. To minimize the time delay, Ding *et al.* [24] investigated three multiple access schemes – OMA, pure NOMA, and hybrid NOMA – for MEC offloading in a two-users scenario. Furthermore, the authors of [25] extended the NOMA-based computation offloading philosophy to a general multi-users scenario, where both task offloading and result retrieval relied on NOMA. Pei *et al.* [26] studied secure NOMA-based computation offloading in the presence of eavesdroppers. To maximize the total transmission rate, the authors of [27] investigated the scenario where a host device offloaded its latency-constrained computation task to the surrounding cooperative devices by combining both non-orthogonal downlink and uplink transmissions. The authors of [28] and [29] applied NOMA-based computation offloading in vehicular networks, where both the macrocells BSs and RSUs may act as the computing nodes. However, these static NOMA-based computation offloading schemes are not suitable for the platoons considered in the face of dynamic task arrival.

For *dynamic NOMA-based computation offloading*, both the channel fluctuations and dynamic task arrivals are considered. The authors of [18] and [30] investigated in the multi-user NOMA uplink computation offloading and multi-server aided downlink NOMA computation offloading, respectively. The classic Lyapunov optimization method was used for converting the long-term utility optimization problem into an online

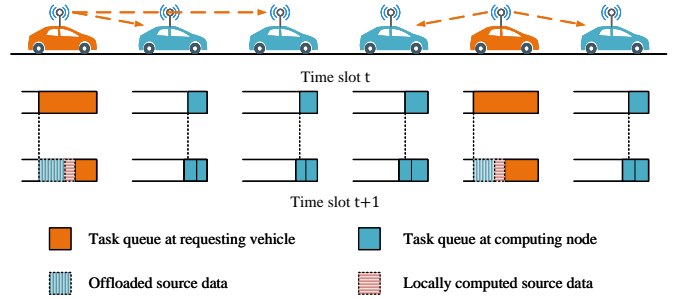


Fig. 1. The considered vehicular platoon system.

optimization problem in both these studies. As a further advance, the authors of [31] considered both the long-term and short-term system behavior, where machine learning based prediction and Lyapunov optimization were adopted, respectively. Qian *et al.* [32] investigated a multi-task multi-access MEC system, where deep reinforcement learning was used for finding near-optimal offloading solutions for time-varying channel realizations. However, these treatises have assumed perfect channel state information (CSI), which is impractical especially in vehicular scenarios, since the movement of wireless terminals will impact the CSI acquisition accuracy.

Hence, by taking both the dynamic channel environment as well as dynamic task arrival and realistic imperfect channel estimation into account, we construct a dynamic cooperative NOMA-based computation offloading scheme for a vehicular platoon. Both the computation offloading and communication resource allocation are optimized for all platoon members according to the near-instantaneous channel state and task queues at the vehicles. NOMA-based computation offloading is considered among all platoon members, and no other edge computing servers are involved in the scenario considered.

## III. SYSTEM MODEL AND PROBLEM FORMULATION

### A. System Overview

As shown in Fig. 1, we consider a steadily moving vehicular platoon on the highway. Denote vehicles within the platoon as  $\mathcal{K} = \{1, 2, \dots, k, \dots, K\}$  with  $K$  representing the number of vehicles, which can partially or fully offload their computation-intensive tasks to other platoon members. On the other hand, they can also serve as computing nodes processing the tasks offloaded by other platoon members to them. To differentiate the two roles of each vehicle, we denote the computing node set as  $\mathcal{N} = \{1, 2, \dots, n, \dots, N\}$  with  $N = K$ . The distance between any two adjacent vehicles in the platoon is assumed to be equal and it is denoted by  $d_v$ . According to the intelligent driver model (IDM) of [33], [34], the equilibrium intra-platoon spacing is given by

$$d_v = \frac{d_0 + vt_0}{\sqrt{1 - \left(\frac{v}{v_m}\right)^4}}, \quad (1)$$

where  $d_0$  is the minimum intra-platoon spacing,  $v$  is the driving velocity,  $t_0$  is the desired time headway, and  $v_m$  is the maximum speed.

We divide the timeline into successive time slot (TSs) according to the channel's coherence time, which are denoted by  $\mathcal{T} = \{1, 2, \dots, t, \dots\}$ . The duration of a TS is denoted by  $\tau$ . Furthermore, the channel quality at TSs is assumed to remain time-invariant and be uncorrelated with that of other TSs. Each vehicle has some computation-intensive tasks. We assume that the arrival of such tasks follows Poisson distribution with an arrival rate of  $\lambda$ , and the data size of the tasks follows a uniform distribution  $\theta_k(t) \sim \mathcal{U}(\theta_k^{\min}, \theta_k^{\max})$ . Usually, computation-intensive tasks only arrive infrequently, hence they tend to have a long inter-arrival time interval, which indicates that  $\theta_k(t)$  equals 0 in most TSs.

In each TS, the specific vehicles having heavy computational burden can offload parts of their tasks to other vehicles by relying on the non-orthogonal downlink and can execute parts of their tasks locally. Meanwhile, some vehicles receive the offloaded tasks and push it into their task buffer. These tasks are then executed in the following TS.

### B. NOMA Offloading

In this subsection, we will elaborate on the process of data transmission between the requesting vehicle and the computing nodes. Upon taking the channel estimation errors into account in the platoon [35], the actual channel coefficient can be written as

$$h_{kn}(t) = \hat{h}_{kn}(t) + \Delta h_{kn}(t), \quad (2)$$

with  $\Delta h_{kn} \sim \mathcal{CN}(0, \sigma_h^2)$ . Under the assumption of uncorrelated Rayleigh fading, the estimated channel coefficient  $\hat{h}_{kn}(t)$  and the channel estimation error  $\Delta h_{kn}(t)$  remain time-invariant during a TS, but they vary randomly and independently between consecutive TSs. Moreover, the estimated channel coefficient  $\hat{h}_{kn}$  can be modeled by [35]

$$\hat{h}_{kn}(t) = \sqrt{G}(d_{kn})^{-\frac{\phi}{2}} g_{kn}(t), \quad (3)$$

where  $G$  is the path-loss factor,  $d_{kn}$  is the distance between vehicle  $k$  and computing node  $n$ ,  $\phi$  is the path-loss exponent, and  $g_{kn}$  reflects the small-scale fading, which obeys a complex Gaussian distribution with zero mean and unit variance. The distance between vehicle  $k$  and computing node  $n$  can be further written as  $d_{kn} = |k - n|d_v$ .

Let us consider the task offloading of vehicle  $k$ . Assume that the computing node  $n$  ( $n \neq k$ ) receives the superimposed NOMA signal from the requesting vehicle  $k$ , which is formulated as

$$\begin{aligned} r_{kn}(t) &= \left( \hat{h}_{kn}(t) + \Delta h_{kn}(t) \right) \sum_{i \in \mathcal{N}} \sqrt{p_{ki}(t)} x_{ki} + \varpi_{kn} \\ &= \hat{h}_{kn}(t) \sqrt{p_{kn}(t)} x_{kn} + \Delta h_{kn}(t) \sum_{i \in \mathcal{N}} \sqrt{p_{ki}(t)} x_{ki} \\ &\quad + \hat{h}_{kn}(t) \sum_{i \in \mathcal{N} \setminus \{n\}} \sqrt{p_{ki}(t)} x_{ki} + \varpi_{kn}, \end{aligned} \quad (4)$$

where  $p_{ki}(t)$  denotes the power allocated to transmit source data from vehicle  $k$  to computing node  $i$  in TS  $t$ ,  $x_{ki}$  with  $\mathbb{E}[|x_{ki}|^2] = 1$  denotes the signal transmitted from vehicle  $k$  to computing node  $i$  and  $\varpi_{kn}$  is the complex additive white

Gaussian noise process having a power spectral density  $N_0$ . It is noted that  $p_{ki}(t) = 0$  indicates that the computing task at vehicle  $k$  is not offloaded to computing node  $i$  in TS  $t$ , and  $p_{kk}(t) = 0$  holds for all vehicles.

The signal to interference plus noise ratio (SINR) at the target vehicles is formulated in (5), shown at the top of the next page. The value  $w_k(t)$  is the bandwidth allocated to vehicle  $k$ , and the indicator function  $\mathbb{I}(\cdot)$  is defined as

$$\mathbb{I}(|\hat{h}_{ki}(t)|^2 > |\hat{h}_{kn}(t)|^2) = \begin{cases} 1, & \text{if } |\hat{h}_{ki}(t)|^2 > |\hat{h}_{kn}(t)|^2, \\ 0, & \text{otherwise.} \end{cases} \quad (6)$$

Moreover, the frequency band occupied by different vehicles for offloading their task is assumed to be orthogonal, which indicates that the constraint of  $\sum_{k \in \mathcal{K}} w_k(t) \leq W_0$  with  $W_0$  denoting the total available bandwidth holds. Then the achievable data rate of offloading data from vehicle  $k$  to computing node  $n$  in TS  $t$  is

$$R_{kn}^{\text{achi}}(t) = w_k(t) \cdot \log_2 [1 + \Gamma_{kn}(t)]. \quad (7)$$

To ensure reliable transmissions among vehicles, the outage probability (OP) must not exceed a given threshold. Specifically, the transmission data rate  $R_{kn}(t)$  should satisfy

$$\Pr \{ R_{kn}^{\text{achi}}(t) \leq R_{kn}(t) \} \leq \eta_0, \quad (8)$$

where  $\eta_0 \in (0, 1]$  specifies the maximum tolerable OP.

Considering the relatively small size of computation results, we ignore the data rate requirement of retrieving the results from the corresponding computing nodes. Then, the energy consumption during this offloading process can be formulated as

$$E_k^{\text{off}}(t) = \sum_n p_{kn}(t) \tau. \quad (9)$$

### C. Local Computation Model

Here, we briefly introduce the computational model of [36] used for characterizing the computing capability of vehicles. The maximum operating frequency (in CPU cycles per second) of all vehicles is assumed to be equal and it is denoted by  $f_m$ . Leveraging dynamic voltage and frequency scaling techniques, the operating frequency can be dynamically adjusted according to the current computing burden. We denote the clock-frequency (in CPU cycles per second) at vehicle  $k$  in TS  $t$  as  $f_k(t)$ . Then the locally computed data during TS  $t$  can be written as

$$D_k^{\text{comp}}(t) = \frac{f_k(t)}{\epsilon_k} \tau, \quad (10)$$

where  $\epsilon_k$  is the computational workload reflecting the number of CPU cycles required for processing a single input bit.

Furthermore, according to the well-established computational model of [37], the energy consumption of the local computing at vehicle  $k$  in TS  $t$  is formulated as

$$E_k^{\text{comp}}(t) = \xi_k f_k^3(t) \tau, \quad (11)$$

where  $\xi_k$  is the energy efficiency coefficient determined by the architecture of the processor used at vehicle  $k$ .

Therefore, the total energy consumption of the platoon in

$$\Gamma_{kn}(t) = \frac{p_{kn}(t)|\hat{h}_{kn}(t)|^2}{|\hat{h}_{kn}(t)|^2 \sum_{i \in \mathcal{N} \setminus \{n\}} p_{ki}(t) \mathbb{I}(|\hat{h}_{ki}(t)|^2 > |\hat{h}_{kn}(t)|^2) + |\Delta h_{kn}(t)|^2 \sum_{i \in \mathcal{N}} p_{ki}(t) + w_k(t)N_0}. \quad (5)$$

TS  $t$  is formulated as

$$E^{\text{total}}(t) = \sum_{k \in \mathcal{K}} E_k^{\text{total}}(t) = \sum_{k \in \mathcal{K}} \left[ \sum_n p_{kn}(t)\tau + \xi_k f_k^3(t)\tau \right]. \quad (12)$$

#### D. Problem Formulation

Considering an individual vehicle  $k$ , the data  $D_k(t)$  that departed from the task queue includes the offloading data  $D_k^{\text{off}}(t)$  and the locally executed data  $D_k^{\text{comp}}(t)$  in TS  $t$ . Meanwhile, for the computing node  $k$ , the data that arrived at the input of the task queue  $A_k(t)$  is comprised of the data  $A_k^{\text{rece}}(t)$  received from other vehicles and the newly generated task  $A_k^{\text{gene}}(t)$  in TS  $t$ . To be specific,  $D_k(t)$  and  $A_k(t)$  can be further expressed as

$$D_k(t) = D_k^{\text{off}}(t) + D_k^{\text{comp}}(t) = \sum_{n \in \mathcal{N} \setminus \{k\}} R_{kn}\tau + \frac{f_k(t)}{\epsilon_k}\tau \quad (13)$$

and

$$A_k(t) = A_k^{\text{rece}}(t) + A_k^{\text{gene}}(t) = \sum_{i \in \mathcal{K} \setminus \{k\}} R_{ik}\tau + \theta_k(t). \quad (14)$$

Assume that each vehicle is equipped with sufficient storage to store the source data to be processed and the length of the task queue at vehicle  $k$  in TS  $t$  is denoted by  $Q_k(t)$ . Then the associated computing task queue is formulated as

$$Q_k(t+1) = [Q_k(t) - D_k(t)]^+ + A_k(t), \quad (15)$$

where  $[x]^+$  equals the larger one between 0 and  $x$ . To ensure the successful completion of each computation-intensive task within a finite delay, the task queue should satisfy

$$\lim_{t \rightarrow \infty} \frac{\mathbb{E}[Q_k(t)]}{t} = 0, \quad \forall k \in \mathcal{K}. \quad (16)$$

Considering the limited power supply of the vehicles, the problem to be solved is to minimize the average total energy consumption of the platoon under the constraints of maximum CPU operating frequency, maximum transmit power and the available frequency band, which can be written as

$$\mathcal{P}1: \min_{\mathbf{P}(t), \mathbf{w}(t), \mathbf{f}(t)} \lim_{T \rightarrow \infty} \frac{1}{T} \sum_{t=1}^T E^{\text{total}}(t) \quad (17)$$

$$\text{s.t. } f_k(t) \leq f_m, \quad \forall k \in \mathcal{K}, \forall t \in \mathcal{T}, \quad (17a)$$

$$\sum_{n \in \mathcal{N}} p_{kn}(t) \leq P_0, \quad \forall k \in \mathcal{K}, \forall t \in \mathcal{T}, \quad (17b)$$

$$\sum_{k \in \mathcal{K}} w_k(t) \leq W_0, \quad \forall t \in \mathcal{T}, \quad (17c)$$

$$\lim_{t \rightarrow \infty} \frac{\mathbb{E}[Q_k(t)]}{t} = 0, \quad \forall k \in \mathcal{K}, \quad (17d)$$

$$\Pr\{R_{kn}^{\text{achi}}(t) \leq R_{kn}(t)\} = \eta_0, \quad \forall k \in \mathcal{K}, \forall n \in \mathcal{N}, \forall t \in \mathcal{T}, \quad (17e)$$

where the optimization parameters  $\mathbf{P}(t)$ ,  $\mathbf{w}(t)$  and  $\mathbf{f}(t)$  are represented by a matrix or vector holding the transmit power, frequency band and CPU clock-frequency of all vehicles in TS  $t$ , which are given by

$$\begin{cases} \mathbf{P}(t) = [\mathbf{p}_1(t), \mathbf{p}_2(t), \dots, \mathbf{p}_K(t)], \\ \mathbf{w}(t) = [w_1(t), w_2(t), \dots, w_K(t)], \\ \mathbf{f}(t) = [f_1(t), f_2(t), \dots, f_K(t)]. \end{cases}$$

The vector  $\mathbf{p}_k(t)$  can be further written as  $\mathbf{p}_k(t) = [p_{k1}(t), p_{k2}(t), \dots, p_{kn}(t), \dots, p_{kN}(t)]^T$ .

Constraints (17a) and (17b) reflect that the processing frequency and transmit power of each vehicle must not exceed their corresponding maximum value. Constraint (17c) guarantees that the sum of occupied bandwidth for all vehicles is less than the available frequency bandwidth of the platooning system. Constraint (17d) ensures that all tasks generated by the vehicles can be completed within finite latency. Finally, constraint (17e) indicates that the OP of none of the vehicles exceeds a given threshold.

#### IV. ALGORITHM DESIGN

The problem  $\mathcal{P}1$  of (17) satisfies the long-term stability of the task queues, but reliable decisions have to be made also for each TS. The objective function (OF) and its parameters consider different timescales. Therefore, the long-term OF and long-term constraints have to be projected into each TS for tackling the problem in (17). In this context, the Lyapunov optimization method of [20] constitutes a powerful tool of constructing a new OF, while ensuring that all long-term objectives are reflected. As a benefit, the transformed problem can be solved by only considering the current network state in each TS.

We now proceed by first reformulating the original optimization task of (17) into a new online optimization problem based on the Lyapunov optimization method, where the system decisions  $\mathbf{P}(t)$ ,  $\mathbf{w}(t)$ , and  $\mathbf{f}(t)$  are determined solely by the system state of the current TS. The general procedures of converting this kind of dynamic optimization problem into an online optimization problem by leveraging Lyapunov's method are summarized as follows:

- **Step 1:** Define the Lyapunov function that involves all actual or virtual queues constructed to reflect the current state of them, such as the task queues of all vehicles in our model considered.
- **Step 2:** The Lyapunov drift is appropriately adjusted for guaranteeing the stability of the queues constructed in Step 1. For example, the Lyapunov drift will be increased when the task queues of the vehicles become too long.
- **Step 3:** The Lyapunov drift-plus-penalty function regarded as the new optimization objective is formulated

by appropriately weighting the conditional Lyapunov drift and the primary optimization OF.

Based on the above steps, the long-term utility and long-term constraints can be removed from the problem formulated, which simplifies the algorithmic design. Furthermore, the performance gap between the optimal solution of the primary problem and the solution of the reformulated problem can be rendered arbitrarily small, as proven in [20]. Here, we adopt the Lyapunov-based method of [20] for designing an online algorithm to approximately apportion the computing and communication resources for all vehicles in the vehicular platoon.

#### A. Problem Transformation

Specifically, the computing task queues of the vehicles formulated in (15) for the platoon are further elaborated on. Denote all task queues as  $\Theta(t) = [Q_1(t), Q_2(t), \dots, Q_K(t)]$ . Then the Lyapunov function is defined by

$$L(\Theta(t)) = \frac{1}{2} \sum_{k \in \mathcal{K}} Q_k^2(t), \quad (18)$$

while the Lyapunov drift can be expressed as

$$\Delta(\Theta(t)) = L[\Theta(t+1)] - L[\Theta(t)]. \quad (19)$$

Then, the Lyapunov drift-plus-penalty function is formulated as

$$\Delta_V(\Theta(t)) = \mathbb{E} [\Delta(\Theta(t)) + VE^{\text{total}}(t) | \Theta(t)], \quad (20)$$

where  $V$  is a non-negative weight reflecting the tradeoff between system utility and queue stability.

**Lemma 1.** *For arbitrary feasible  $\mathbf{P}(t)$ ,  $\mathbf{w}(t)$ ,  $\mathbf{f}(t)$ , the Lyapunov drift-plus-penalty function is upper bounded by*

$$\begin{aligned} \Delta_V(\Theta(t)) &\leq \Phi + \mathbb{E} \left[ \sum_{k \in \mathcal{K}} Q_k(t) [A_k(t) - D_k(t)] | \Theta(t) \right] \\ &\quad + \mathbb{E} [VE^{\text{total}}(t) | \Theta(t)], \end{aligned} \quad (21)$$

where  $\Phi$  is a constant. The proof is relegated to Appendix A for retaining the flow of our arguments.

Then, the primary optimization problem  $\mathcal{P}1$  of (17) can be transformed into minimizing the upper bound of the Lyapunov drift-plus-penalty function, which is formulated as

$$\mathcal{P}2: \min_{\mathbf{P}(t), \mathbf{w}(t), \mathbf{f}(t)} \sum_{k \in \mathcal{K}} Q_k(t) [A_k(t) - D_k(t)] + VE^{\text{total}}(t) \quad (22)$$

s.t. (17a), (17b), (17c) and (17e).

Before elaborating on the transformed optimization problem, we first derive the achievable transmission rate  $R_{kn}(t)$  based on the constraint (17e), which is given in the following lemma.

**Lemma 2.** *The transmission data rate between vehicle  $k$  and computing node  $n$  under our OP constraint can be expressed*

as

$$\begin{aligned} R_{kn}(t) &= w_k(t) \log_2 \left( 1 + \frac{p_{kn}(t) |\hat{h}_{kn}(t)|^2}{H(\mathbf{p}_k(t), w_k(t)) - \ln(\eta_0) \sigma_h^2 \sum_{i \in \mathcal{K}} p_{ki}(t)} \right), \end{aligned} \quad (23)$$

where the function  $H[\mathbf{p}_k(t), w_k(t)]$  is defined as

$$\begin{aligned} H[\mathbf{p}_k(t), w_k(t)] &= |\hat{h}_{kn}(t)|^2 \sum_{i \in \mathcal{N} \setminus \{n\}} p_{ki}(t) \mathbb{I}(|\hat{h}_{ki}(t)|^2 > |\hat{h}_{kn}(t)|^2) + w_k(t) N_0. \end{aligned}$$

The proof is relegated to Appendix B for retaining the flow of our arguments.

Upon substituting (12), (13), (14), and (23) into the OF of problem  $\mathcal{P}2$ , the detailed expression is given in (24), shown at the top of the next page. Here, we represent the OF in a more concise way as follows,

$$\begin{aligned} O(\mathbf{P}(t), \mathbf{w}(t), \mathbf{f}(t)) &= \sum_{k \in \mathcal{K}} Q_k(t) [A_k(t) - D_k(t)] + VE^{\text{total}}(t) \\ &= \sum_{k \in \mathcal{K}} Q_k(t) \theta_k(t) + O_1[\mathbf{f}(t)] + O_2[\mathbf{P}(t), \mathbf{w}(t)]. \end{aligned} \quad (25)$$

The first subitem in (25) is a deterministic value in each TS, and it does not affect the system decisions  $[\mathbf{P}(t), \mathbf{w}(t), \mathbf{f}(t)]$ . Then, we can decouple the optimization problem  $\mathcal{P}2$  into the subproblems of  $\mathcal{P}2.1$  and  $\mathcal{P}2.2$ , where  $\mathcal{P}2.1$  minimizes the OF  $O_1[\mathbf{f}(t)]$  in terms of  $\mathbf{f}(t)$ , while  $\mathcal{P}2.2$  minimizes the OF  $O_2[\mathbf{P}(t), \mathbf{w}(t)]$  in terms of  $\mathbf{P}(t)$  and  $\mathbf{w}(t)$ . In the following part, we will deal with these two subproblems independently.

#### B. Computing Resource Allocation

The computing resource allocation subproblem is stated as

$$\begin{aligned} \mathcal{P}2.1: \min_{\mathbf{f}(t)} O_1[\mathbf{f}(t)] \\ \text{s.t.} \quad (17a). \end{aligned} \quad (26)$$

The property of strong duality holds for the optimization problem  $\mathcal{P}2.1$ . Therefore, the optimal processing frequency can be obtained by satisfying the Karush–Kuhn–Tucker (KKT) conditions. The associated Lagrangian of  $\mathcal{P}2.1$  is given by

$$\mathcal{L}[\mathbf{f}(t), \lambda] = O_1[\mathbf{f}(t)] + \sum_{k \in \mathcal{K}} \lambda_k [f_k(t) - f_m]. \quad (27)$$

Then, the KKT conditions are formulated as

$$\frac{\partial \mathcal{L}[\mathbf{f}(t), \lambda]}{\partial f_k(t)} = 3V\xi_k f_k^2(t) - \frac{Q_k(t)}{\epsilon_k} + \lambda_k = 0, \quad \forall k \in \mathcal{K}, \quad (28)$$

$$\lambda_k [f_k(t) - f_m] = 0, \quad \forall k \in \mathcal{K}, \quad (29)$$

$$f_k(t) - f_m \leq 0, \quad \forall k \in \mathcal{K}, \quad (30)$$

$$\lambda_k \geq 0, \quad \forall k \in \mathcal{K}, \quad (31)$$

$$\begin{aligned}
& \sum_{k \in \mathcal{K}} Q_k(t) [A_k(t) - D_k(t)] + V E^{\text{total}}(t) \\
&= \sum_{k \in \mathcal{K}} Q_k(t) \left[ \sum_{n \in \mathcal{N} \setminus \{k\}} R_{nk} \tau + \theta_k(t) - \sum_{n \in \mathcal{N} \setminus \{k\}} R_{kn} \tau - \frac{f_k(t)}{\epsilon_k} \tau \right] + V \sum_{k \in \mathcal{K}} \left[ \xi_k f_k^3(t) \tau + \sum_{n \in \mathcal{N}} p_{kn}(t) \tau \right] \\
&= \sum_{k \in \mathcal{K}} Q_k(t) \theta_k(t) + \sum_{k \in \mathcal{K}} \sum_{n \in \mathcal{N} \setminus \{k\}} [Q_n(t) - Q_k(t)] R_{kn} \tau + V \sum_{k \in \mathcal{K}} \sum_{n \in \mathcal{N}} p_{kn}(t) \tau + V \sum_{k \in \mathcal{K}} \xi_k f_k^3(t) \tau - \sum_{k \in \mathcal{K}} Q_k(t) \frac{f_k(t)}{\epsilon_k} \tau \\
&= \sum_{k \in \mathcal{K}} Q_k(t) \theta_k(t) + \underbrace{V \sum_{k \in \mathcal{K}} \xi_k f_k^3(t) \tau - \sum_{k \in \mathcal{K}} Q_k(t) \frac{f_k(t)}{\epsilon_k} \tau}_{O_1(\mathbf{f}(t))} \\
&\quad + \underbrace{\sum_{k \in \mathcal{K}} \sum_{n \in \mathcal{N}} \tau w_k(t) [Q_n(t) - Q_k(t)] \log_2 \left( 1 + \frac{p_{kn}(t) |\hat{h}_{kn}(t)|^2}{H(\mathbf{p}_k(t), w_k(t)) - \ln(\eta_0) \sigma_h^2 \sum_{i \in \mathcal{K}} p_{ki}(t)} \right)}_{O_2(\mathbf{P}(t), \mathbf{w}(t))} + V \sum_{k \in \mathcal{K}} \sum_{n \in \mathcal{N}} p_{kn}(t) \tau. \quad (24)
\end{aligned}$$

which leads to

$$f_k^*(t) = \min \left\{ \sqrt{\frac{Q_k(t)}{3V\xi_k\epsilon_k}}, f_m \right\}. \quad (32)$$

### C. Communication Resource Allocation

The communication resource allocation subproblem is formulated as

$$\begin{aligned}
\mathcal{P}2.2: \quad & \min_{\mathbf{P}(t), \mathbf{w}(t)} O_2[\mathbf{P}(t), \mathbf{w}(t)] \\
\text{s.t.} \quad & (17b) \text{ and } (17c).
\end{aligned} \quad (33)$$

It can be directly derived from the definition of  $O_2[\mathbf{P}(t), \mathbf{w}(t)]$  given in (24) that the optimal power allocation satisfies

$$p_{kn}^*(t) = 0, \text{ if } Q_k(t) < Q_n(t), \quad (34)$$

and the optimal spectral resource allocation satisfies

$$w_k^*(t) = 0, \text{ if } \sum_{n \in \mathcal{N}} p_{kn}(t) = 0. \quad (35)$$

These results indicate that computing task offloading only occurs, when the task queue  $Q_k(t)$  of vehicle  $k$  is longer than the queue  $Q_n(t)$  at computing node  $n$ . With the aid of (34) and (35), the OF of problem  $\mathcal{P}2.2$  is shown to be non-convex. In the following, we adopt the BSUM approach to solve the problem [21].

Firstly, we rewrite the expression of  $O_2[\mathbf{P}(t), \mathbf{w}(t)]$  in (36), shown at the top of this page. Then, we can find from (24) and (36) that  $O_2[\mathbf{P}(t), \mathbf{w}(t)]$  is convex in terms of  $\mathbf{w}(t)$ , when the power allocation  $\mathbf{P}(t)$  is fixed, and the OF is a sum of a convex function  $F_+[\mathbf{P}(t), \mathbf{w}(t)]$  and a concave function  $F_-[\mathbf{P}(t), \mathbf{w}(t)]$ , when the spectrum allocation  $\mathbf{w}(t)$  is fixed.

Hence, the approximate functions required for updating  $\mathbf{p}_k(t)$  and  $\mathbf{w}(t)$  are given by

$$\begin{aligned}
& g_k(\mathbf{p}_k(t) | \bar{\mathbf{w}}(t), \bar{\mathbf{P}}(t)) \\
&= F_+([\bar{\mathbf{p}}_1(t), \dots, \mathbf{p}_k(t), \dots, \bar{\mathbf{p}}_K(t)], \bar{\mathbf{w}}(t)) \\
&\quad + \nabla_{\mathbf{p}_k(t)} F_- (\bar{\mathbf{w}}(t), \bar{\mathbf{P}}(t))^T (\mathbf{p}_k(t) - \bar{\mathbf{p}}_k(t))
\end{aligned} \quad (37)$$

and

$$l[\mathbf{w}(t) | \bar{\mathbf{w}}(t), \bar{\mathbf{P}}(t)] = O_2(\bar{\mathbf{P}}(t), \mathbf{w}(t)), \quad (38)$$

respectively. After these approximations, the functions  $g_k[\mathbf{p}_k(t)]$  for  $\forall k \in \mathcal{K}$  and  $l[\mathbf{w}(t) | \bar{\mathbf{w}}(t)]$  are both convex.

The updated values of  $\mathbf{p}_k(t)$  and  $\mathbf{w}(t)$  are obtained by solving the following convex problems,

$$\bar{\mathbf{p}}_k(t) = \arg \min_{\mathbf{p}_k(t)} g_k(\mathbf{p}_k(t) | \bar{\mathbf{w}}(t), \bar{\mathbf{P}}(t)), \text{ s.t. } \sum_{n \in \mathcal{N}} p_{kn}(t) \leq P_0 \quad (39)$$

and

$$\bar{\mathbf{w}}(t) = \arg \min_{\mathbf{w}(t)} O_2(\bar{\mathbf{P}}(t), \mathbf{w}(t)), \text{ s.t. } \sum_{k \in \mathcal{K}} w_k(t) \leq W_0, \quad (40)$$

respectively. However, it still remains a challenge to obtain the analytical solutions of the problem stated in (39) and (40). Here, we adopt the off-the-shelf convex optimization toolbox CVX [38] to solve these two convex problems. The BSUM algorithm conceived for solving the subproblem  $\mathcal{P}2.2$  is summarized in Algorithm 1.

---

#### Algorithm 1 BSUM algorithm for subproblem $\mathcal{P}2.2$

---

##### Input:

A feasible point  $(\bar{\mathbf{w}}(t), \bar{\mathbf{P}}(t))$ ;

##### Output:

Optimal power allocation  $\mathbf{P}^*(t)$ ;

Optimal spectrum resource allocation  $\mathbf{w}^*(t)$ ;

##### 1: repeat

2: **for**  $k \in \{1, 2, \dots, K\}$  **do**

3: Updating  $\bar{\mathbf{p}}_k(t)$  by solving (39);

4: **end for**

5: Updating  $\bar{\mathbf{w}}(t)$  by solving (40);

6: **until** The variation of the value of  $O_2(\bar{\mathbf{P}}(t), \bar{\mathbf{w}}(t))$  before updating and after updating is less than  $\delta_0$ .

7:  $\mathbf{P}^*(t) = \bar{\mathbf{P}}(t)$ ,  $\mathbf{w}^*(t) = \bar{\mathbf{w}}(t)$ .

---

$$\begin{aligned}
O_2[\mathbf{P}(t), \mathbf{w}(t)] = & \underbrace{\sum_{k \in \mathcal{K}} \sum_{n \in \mathcal{N}} \tau w_k(t) [Q_k(t) - Q_n(t)] \log_2 \left( H(\mathbf{p}_k(t), w_k(t)) + \ln(1/\eta_0) \sigma_h^2 \sum_{i \in \mathcal{N}} p_{ki}(t) \right)}_{F_-(\mathbf{P}(t), \mathbf{w}(t))} \\
& - \underbrace{\sum_{k \in \mathcal{K}} \sum_{n \in \mathcal{N}} \tau w_k(t) [Q_k(t) - Q_n(t)] \log_2 \left( H(\mathbf{p}_k(t), w_k(t)) + \ln(1/\eta_0) \sigma_h^2 \sum_{i \in \mathcal{N}} p_{ki}(t) + p_{kn}(t) |\hat{h}_{kn}(t)|^2 \right)}_{F_+(\mathbf{P}(t), \mathbf{w}(t))} + V \sum_{k \in \mathcal{K}} \sum_{n \in \mathcal{N}} p_{kn}(t) \tau.
\end{aligned} \tag{36}$$

TABLE I  
SIMULATION PARAMETERS

Parameter	Value
Minimum intra-platoon spacing $d_0$	3.0 m
Time headway $t_0$	1.5 s
Maximum driving speed $v_m$	180 km/h
Computation workload $\epsilon_k$	40
Energy coefficient $\xi_k$	$1 \times 10^{-27}$
Time interval $\tau$	1 ms
Maximum operating frequency $f_m$	1 GHz
Constant path-loss factor $G$	-31.5 dB
Path-loss exponent $\phi$	2
Noise power spectral density $N_0$	-174 dBm/Hz
Maximum transmit power of vehicles $P_0$	35 dBm
Bandwidth $W_0$	20 MHz
Arrival rate $\lambda$	1/30
Lower bound of generated data $\theta_k^{\min}$	$5 \times 10^5$ bits
Upper bound of generated data $\theta_k^{\max}$	$6 \times 10^5$ bits
Number of vehicles $K$	8

## V. NUMERICAL RESULTS

In this section, we evaluate the performance of the proposed algorithm in the dynamic NOMA-based computation offloading aided platooning system. Unless otherwise stated, the default simulation parameters are set as shown in TABLE I. The average queue length and average energy consumption in TS  $t$  are defined as  $1/(tK) \sum_{i=1}^t \sum_{k \in \mathcal{K}} Q_k(i)$  and  $1/(tK) \sum_{i=1}^t \sum_{k \in \mathcal{K}} E_k^{\text{total}}(i)$ , respectively. For comparison, we choose the OMA-based offloading system and the local computing system as the benchmarks. In the OMA-based counterpart, the bandwidth allocated to each communication mode pair is orthogonal.

First, the convergence of the BSUM algorithm for subproblem  $\mathcal{P}2.2$  is illustrated in Fig. 2. The initial feasible point is obtained by distributing the bandwidth and transmit power to vehicles evenly. The weighting factor  $V$  is set to  $\{1 \times 10^{12}, 1.5 \times 10^{12}, 2 \times 10^{12}\}$ . It can be seen from Fig. 2 that the OF  $O_2[\mathbf{p}(t), \mathbf{w}(t)]$  converges within a small number of iterations under different parameter settings, which validates the convergence of Algorithm 1.

Figure 3 shows the average queue length in different TSs under different offloading schemes. The velocity  $v$  and the weighting factor  $V$  are set to 108 km/h and  $1 \times 10^{12}$ , respectively. Over time, the average queue length converges

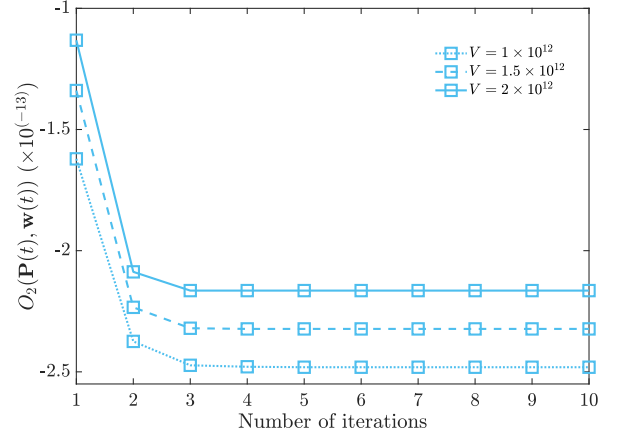


Fig. 2. Convergence of Algorithm 1 evaluated by simulations.

to a specific value. It can be inferred from Fig. 3 that cooperative computation offloading among platoon members through NOMA or OMA reduces the average computing burden of the individual vehicles. Furthermore, the NOMA-based computation offloading scheme significantly outperforms its OMA-based counterpart.

To further illustrate the distribution of  $Q(t)$ , we portray the statistical results over all TSs and all vehicles in Fig. 4 under the same system configuration as in Fig. 3. Observe in Fig. 3 that the queue length is distributed over the range of 0 to  $1.5 \times 10^6$  with an extremely high probability in our NOMA-based computation offloading platoon system, while the range spans from 0 to  $2 \times 10^6$  and from 0 to  $4 \times 10^6$  for the OMA-based offloading scheme and for the local computing scheme, respectively. Explicitly, we conclude from Fig. 4 that NOMA-based computation offloading can guarantee a much lower queue length.

To study the effect of driving velocity on NOMA-based computation offloading, Figure 5 plots the average queue length at the vehicles versus the velocity  $v$  under different offloading schemes. The weighting factor  $V$  is set to  $1 \times 10^{12}$  for all velocities. Intuitively, the average queue length is expected to increase with the velocity  $v$  for both NOMA-based and OMA-based offloading. This is because the spacing among vehicles becomes higher for a higher velocity, which reduces the offloading probability at the same weighting factor  $V$ . Moreover, the performance gap between NOMA-based and OMA-based offloading is reduced upon increasing the velocity

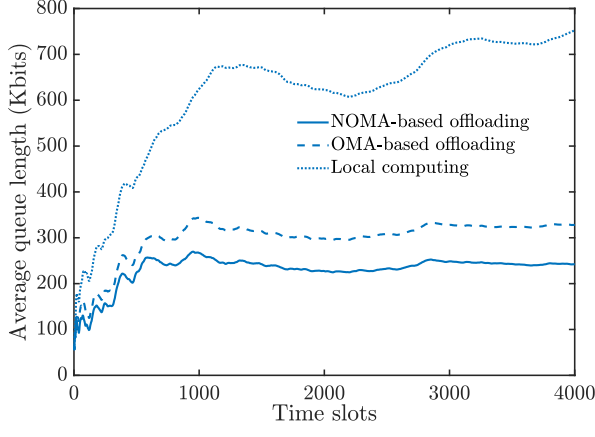


Fig. 3. Average queue length versus the TSs index under different offloading strategies evaluated by simulations.

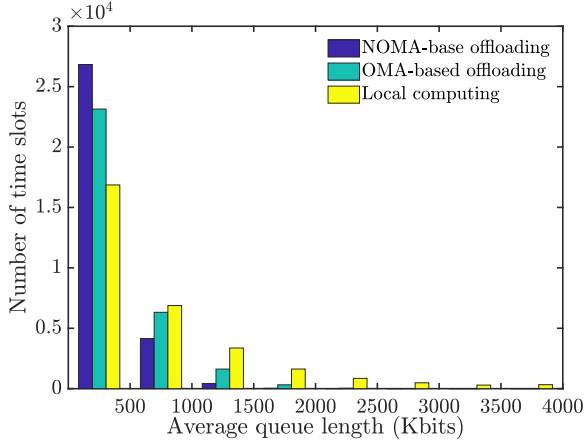


Fig. 4. The distribution of queue length under different offloading strategies evaluated by simulations.

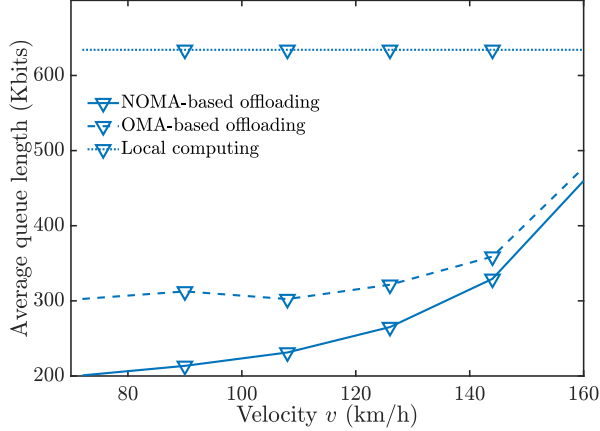


Fig. 5. Average queue length versus driving velocities evaluated by simulations.

$v$ , which would tend to zero for a sufficiently large velocity  $v$ . Explicitly, computation offloading will seldom be used over long distances.

Furthermore, the average energy consumption at the vehicles versus velocity  $v$  under different offloading schemes is

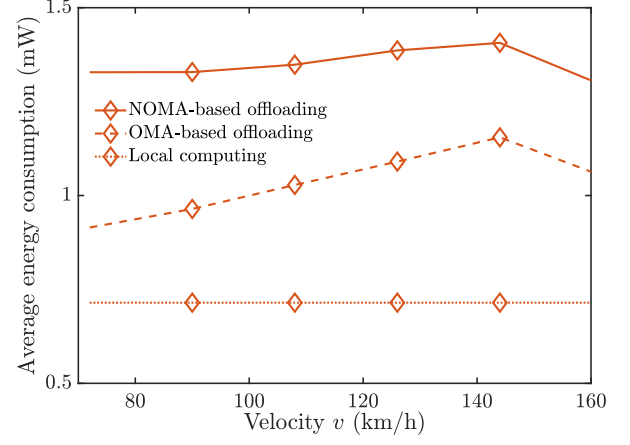


Fig. 6. Average energy consumption versus driving velocities evaluated by simulations.

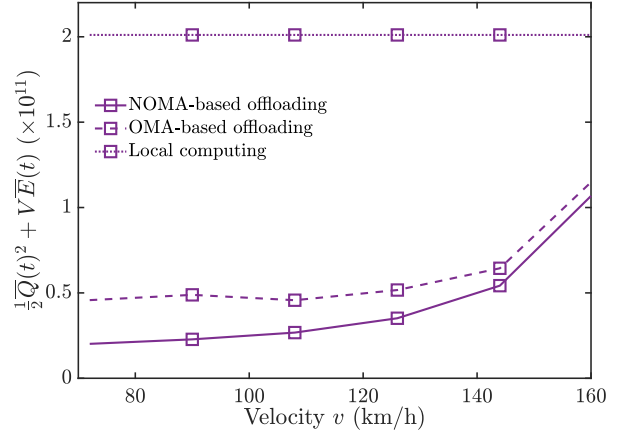


Fig. 7. Weight value versus driving velocities evaluated by simulations.

plotted in Fig. 6. Naturally, the average energy consumption of the local computing scheme is the lowest, because all data is processed locally, which does not require any energy for communications. The NOMA-based offloading scheme conveys more data than OMA, hence it dissipates more energy. Moreover, it can be seen from Fig. 6 that the average energy dissipation will increase first, and then decrease beyond about 140 km/h for both NOMA-based and OMA-based computation offloading. Explicitly, it is increased first, owing to the increased spacing between vehicles, which requires increased transmit power. However, when the velocity is above 140 km/h, the offloading probability will sharply decrease, hence reducing the transmit energy dissipation.

In order to quantify the benefits of NOMA-based computation offloading, we consider the value of  $1/2\bar{Q}(t)^2 + V\bar{E}^{(\text{total})}(t)$  as the metric of quantifying the merits of different offloading schemes, which reflects the queue length vs. energy consumption trade-offs. A smaller value of  $1/2\bar{Q}(t)^2 + V\bar{E}^{(\text{total})}(t)$  indicates a better overall performance. In Fig. 7, we portray the metric versus velocity  $v$ . As expected, the NOMA-based offloading scheme outperforms both the OMA-based offloading scheme and the local computing scheme due to the higher energy efficiency of NOMA. Furthermore,

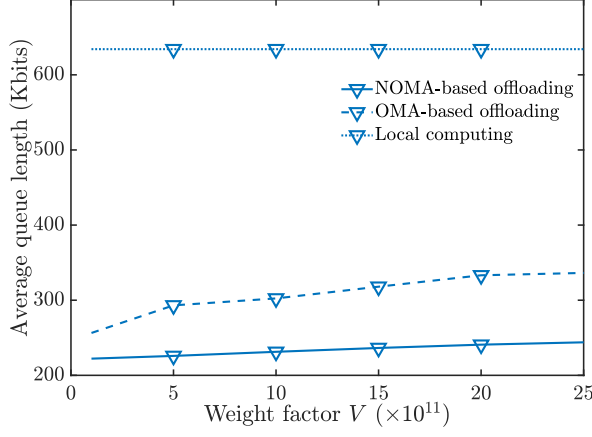


Fig. 8. Average queue length versus weighting factors evaluated by simulations.

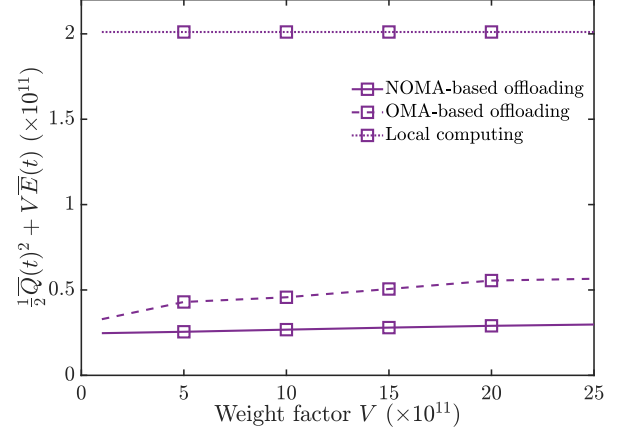


Fig. 10. Average energy consumption versus weighting factors evaluated by simulations.

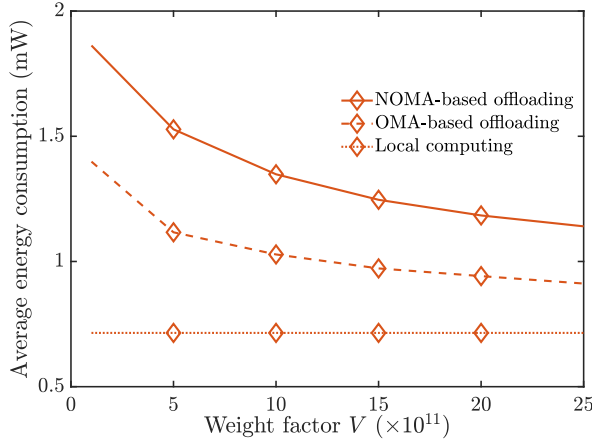


Fig. 9. Average energy consumption versus weighting factors evaluated by simulations.

the performance gap between NOMA-based and OMA-based offloading diminishes upon increasing the velocity.

In Fig. 8, Fig. 9 and Fig. 10, we investigate the influence of the weighting factor  $V$  on the average queue length, average energy consumption and the metric of  $1/2\bar{Q}(t)^2 + V\bar{E}^{(\text{total})}(t)$ , respectively. The velocity  $v$  is set to 108 km/h for all cases. We conclude from Fig. 8 that the average queue length in both NOMA-based and OMA-based offloading will increase, when the weighting factor  $V$  is increased. Nevertheless, compared to its OMA-based counterpart, NOMA-based computation offloading is less sensitive to the weighting factor.

Observe from Fig. 9 that the increase of the weighting factor  $V$  reduces the average energy consumption, in line with the definition of  $V$ . Explicitly, a larger value of  $V$  represents a more stringent energy consumption requirement. Additionally, the average energy consumption of NOMA-based offloading is higher than that of its OMA-based counterpart. Nonetheless, the metric of  $1/2\bar{Q}(t)^2 + V\bar{E}^{(\text{total})}(t)$  in Fig. 10 illustrates the superior performance of the NOMA-based offloading scheme, which manifests itself as a lower average queue length at a given average energy consumption, or as a lower average energy consumption at the same average queue length.

## VI. CONCLUSIONS

A dynamic NOMA-based robust computation offloading scheme was conceived and analyzed for a vehicular platoon. Then the problem of minimizing the long-term energy consumption has been formulated to optimize the offloading decisions and the associated resource allocation. By converting the problem formulated into an online optimization problem, we can solve the primary problem by solely taking into account the current queue state and channel state. Then the classic BSUM method has been adopted for solving the non-convex transformed problem. Our numerical results have shown that NOMA-based computation offloading outperforms both the OMA-based computation offloading and the local computing scheme. Moreover, the effect of driving velocity and the weighting factor of the NOMA-based computation offloading scheme have been investigated. Our simulation results have revealed that a higher velocity and more stringent energy consumption requirement will lengthen the task queues at the vehicles. In our future research, we may conceive a similar scheme for drones flying in formation.

## APPENDIX A PROOF OF LEMMA 1

*Proof:* According to (15), we can proceed as follows:

$$\begin{aligned}
 Q_k^2(t+1) &= \left\{ [Q_k(t) - D_k(t)]^+ + A_k(t) \right\}^2 \\
 &= \left\{ [Q_k(t) - D_k(t)]^+ \right\}^2 + A_k(t)^2 \\
 &\quad + 2A_k(t)[Q_k(t) - D_k(t)]^+ \\
 &\leq [Q_k(t) - D_k(t)]^2 + A_k(t)^2 + 2A_k(t)Q_k(t) \\
 &= Q_k^2(t) + D_k^2(t) + A_k(t)^2 + 2Q_k(t)[A_k(t) - D_k(t)].
 \end{aligned}$$

Then, the Lyapunov drift may be rewritten as

$$\begin{aligned}
\Delta(\Theta(t)) &= \frac{1}{2} \sum_{k \in \mathcal{K}} Q_k^2(t+1) - \frac{1}{2} \sum_{k \in \mathcal{K}} Q_k^2(t) \\
&= \frac{1}{2} \sum_{k \in \mathcal{K}} \{Q_k^2(t+1) - Q_k^2(t)\} \\
&\leq \frac{1}{2} \sum_{k \in \mathcal{K}} \{D_k^2(t) + A_k^2(t) + 2Q_k(t)[A_k(t) - D_k(t)]\} \\
&= \frac{1}{2} \sum_{k \in \mathcal{K}} [D_k^2(t) + A_k^2(t)] + \sum_{k \in \mathcal{K}} Q_k(t)[A_k(t) - D_k(t)] \\
&\leq \Phi + \sum_{k \in \mathcal{K}} Q_k(t)[A_k(t) - D_k(t)],
\end{aligned}$$

where  $\Phi$  is a finite constant denoting the upper bound of  $1/2 \sum_{k \in \mathcal{K}} [D_k^2(t) + A_k^2(t)]$ .

Accordingly, the upper bound of the Lyapunov drift-plus-penalty function is formulated as

$$\begin{aligned}
\Delta_V(\Theta(t)) &= \mathbb{E} [\Delta(\Theta(t)) + VE^{\text{total}}(t) | \Theta(t)] \\
&= \mathbb{E} [\Delta(\Theta(t)) | \Theta(t)] + \mathbb{E} [VE^{\text{total}}(t) | \Theta(t)] \\
&\leq \Phi + \mathbb{E} \left[ \sum_{k \in \mathcal{K}} Q_k(t)[A_k(t) - D_k(t)] | \Theta(t) \right] \\
&\quad + \mathbb{E} [VE^{\text{total}}(t) | \Theta(t)],
\end{aligned} \tag{41}$$

which completes the proof. ■

#### APPENDIX B PROOF OF LEMMA 2

*Proof:* Substituting (5) and (7) into (17e), the OP may be rewritten as (42), shown at the top of this page. According to the assumption that channel estimation error  $\Delta h_{kn}(t)$  obeys a circle symmetric complex Gaussian distribution having a zero mean and variance of  $\sigma_h^2$ , the variable  $z = |\Delta h_{kn}(t)|^2$  follows an exponential distribution with rate parameter of  $1/\sigma_h^2$ . Then, it can be derived from the cumulative distribution function of variable  $z = |\Delta h_{kn}(t)|^2$  that we have:

$$\frac{1}{\sum_{i \in \mathcal{N}} p_{ki}(t)} \left\{ \frac{p_{kn}(t) |\hat{h}_{kn}(t)|^2}{2^{\frac{R_{kn}(t)}{w_k(t)}} - 1} - H(\mathbf{p}_k(t), w_k(t)) \right\} = \ln\left(\frac{1}{\eta_0}\right) \sigma_h^2. \tag{43}$$

Upon applying some routine arithmetic operations to (43), it can be readily shown that the transmission data rate  $R_{kn}(t)$  is formulated as (23). This completes the proof. ■

#### REFERENCES

- [1] K. M. Alam, M. Saini, and A. E. Saddik, "Toward Social Internet of Vehicles: Concept, Architecture, and Applications," *IEEE Access*, vol. 3, pp. 343–357, Mar. 2015.
- [2] J. Contreras-Castillo, S. Zeadally, and J. A. Guerrero-Ibañez, "Internet of Vehicles: Architecture, Protocols, and Security," *IEEE Internet of Things Journal*, vol. 5, no. 5, pp. 3701–3709, Oct. 2018.
- [3] W. Zhang, Z. Zhang, and H. Chao, "Cooperative Fog Computing for Dealing with Big Data in the Internet of Vehicles: Architecture and Hierarchical Resource Management," *IEEE Communications Magazine*, vol. 55, no. 12, pp. 60–67, Dec. 2017.
- [4] Z. Ning, J. Huang, X. Wang, J. J. P. C. Rodrigues, and L. Guo, "Mobile Edge Computing-Enabled Internet of Vehicles: Toward Energy-Efficient Scheduling," *IEEE Network*, vol. 33, no. 5, pp. 198–205, Sept./Oct. 2019.
- [5] J. Feng, Z. Liu, C. Wu, and Y. Ji, "AVE: Autonomous Vehicular Edge Computing Framework with ACO-Based Scheduling," *IEEE Transactions on Vehicular Technology*, vol. 66, no. 12, pp. 10660–10675, Dec. 2017.
- [6] K. Zhang, Y. Mao, S. Leng, Y. He, and Y. ZHANG, "Mobile-Edge Computing for Vehicular Networks: A Promising Network Paradigm with Predictive Off-Loading," *IEEE Vehicular Technology Magazine*, vol. 12, no. 2, pp. 36–44, Jun. 2017.
- [7] Y. Mao, J. Zhang, and K. B. Letaief, "Dynamic Computation Offloading for Mobile-Edge Computing With Energy Harvesting Devices," *IEEE Journal on Selected Areas in Communications*, vol. 34, no. 12, pp. 3590–3605, Dec. 2016.
- [8] X. Hou, Y. Li, M. Chen, D. Wu, D. Jin, and S. Chen, "Vehicular Fog Computing: A Viewpoint of Vehicles as the Infrastructures," *IEEE Transactions on Vehicular Technology*, vol. 65, no. 6, pp. 3860–3873, Jun. 2016.
- [9] C. Huang, R. Lu, and K. R. Choo, "Vehicular Fog Computing: Architecture, Use Case, and Security and Forensic Challenges," *IEEE Communications Magazine*, vol. 55, no. 11, pp. 105–111, Nov. 2017.
- [10] J. Du, F. R. Yu, X. Chu, J. Feng, and G. Lu, "Computation Offloading and Resource Allocation in Vehicular Networks Based on Dual-Side Cost Minimization," *IEEE Transactions on Vehicular Technology*, vol. 68, no. 2, pp. 1079–1092, Feb. 2019.
- [11] I. Sorkhoh, D. Ebrahimi, R. Atallah, and C. Assi, "Workload Scheduling in Vehicular Networks With Edge Cloud Capabilities," *IEEE Transactions on Vehicular Technology*, vol. 68, no. 9, pp. 8472–8486, Sept. 2019.
- [12] D. Jia, K. Lu, J. Wang, X. Zhang, and X. Shen, "A Survey on Platoon-Based Vehicular Cyber-Physical Systems," *IEEE Communications Surveys & Tutorials*, vol. 18, no. 1, pp. 263–284, 1st Quart., 2016.
- [13] T. Zeng, O. Semiari, W. Saad, and M. Bennis, "Joint Communication and Control for Wireless Autonomous Vehicular Platoon Systems," *IEEE Transactions on Communications*, vol. 67, no. 11, pp. 7907–7922, Nov. 2019.
- [14] Z. Ding, X. Lei, G. K. Karagiannis, R. Schober, J. Yuan, and V. K. Bhargava, "A Survey on Non-Orthogonal Multiple Access for 5G Networks: Research Challenges and Future Trends," *IEEE Journal on Selected Areas in Communications*, vol. 35, no. 10, pp. 2181–2195, Oct. 2017.
- [15] A. Kiani and N. Ansari, "Edge Computing Aware NOMA for 5G Networks," *IEEE Internet of Things Journal*, vol. 5, no. 2, pp. 1299–1306, Apr. 2018.
- [16] Y. Liu, F. R. Yu, X. Li, H. Ji, and V. C. M. Leung, "Distributed Resource Allocation and Computation Offloading in Fog and Cloud Networks With Non-Orthogonal Multiple Access," *IEEE Transactions on Vehicular Technology*, vol. 67, no. 12, pp. 12137–12151, Dec. 2018.
- [17] Z. Ding, P. Fan, and H. V. Poor, "Impact of Non-Orthogonal Multiple Access on the Offloading of Mobile Edge Computing," *IEEE Transactions on Communications*, vol. 67, no. 1, pp. 375–390, Jan. 2019.
- [18] N. Nouri, A. Entezari, J. Abouei, M. Jaseemuddin, and A. Anpalagan, "Dynamic Power-Latency Tradeoff for Mobile Edge Computation Offloading in NOMA-Based Networks," *IEEE Internet of Things Journal*, vol. 7, no. 4, pp. 2763–2776, Apr. 2020.
- [19] G. Naik, B. Choudhury, and J. Park, "IEEE 802.11bd & 5G NR V2X: Evolution of Radio Access Technologies for V2X Communications," *IEEE Access*, vol. 7, pp. 70169–70184, May 2019.
- [20] M. J. Neely, "Stochastic Network Optimization with Application to Communication and Queueing Systems," *Synthesis Lectures on Communication Networks*, vol. 3, no. 1, pp. 1–211, Sep. 2010.
- [21] M. Razaviyayn, M. Hong, and Z.-Q. Luo, "A Unified Convergence Analysis of Block Successive Minimization Methods for Nonsmooth Optimization," *SIAM Journal on Optimization*, vol. 23, no. 2, pp. 1126–1153, 2013.
- [22] Y. Pan, M. Chen, Z. Yang, N. Huang, and M. Shikh-Bahaei, "Energy-Efficient NOMA-Based Mobile Edge Computing Offloading," *IEEE Communications Letters*, vol. 23, no. 2, pp. 310–313, Feb. 2019.
- [23] L. Wang, M. Guan, Y. Ai, Y. Chen, B. Jiao, and L. Hanzo, "Beamforming-Aided NOMA Expedites Collaborative Multiuser Computational Offloading," *IEEE Transactions on Vehicular Technology*, vol. 67, no. 10, pp. 10027–10032, Oct. 2018.
- [24] Z. Ding, D. W. K. Ng, R. Schober, and H. V. Poor, "Delay Minimization for NOMA-MEC Offloading," *IEEE Signal Processing Letters*, vol. 25, no. 12, pp. 1875–1879, Dec. 2018.
- [25] Y. Wu, L. P. Qian, K. Ni, C. Zhang, and X. Shen, "Delay-Minimization Nonorthogonal Multiple Access Enabled Multi-User Mobile Edge Computation Offloading," *IEEE Journal of Selected Topics in Signal Processing*, vol. 13, no. 3, pp. 392–407, Jun. 2019.

$$\begin{aligned}
\Pr \{ R_{kn}^{\text{achi}}(t) \leq R_{kn}(t) \} &= \Pr \{ w_k(t) \log_2 (1 + \Gamma_{kn}(t)) \leq R_{kn}(t) \} = \Pr \left\{ \Gamma_{kn}(t) \leq 2^{\frac{R_{kn}(t)}{w_k(t)}} - 1 \right\} \\
&= \Pr \left\{ |\Delta h(t)|^2 \geq \frac{1}{\sum_{i \in \mathcal{N}} p_{ki}(t)} \left\{ \frac{p_{kn}(t) |\hat{h}_{kn}(t)|^2}{2^{\frac{R_{kn}(t)}{w_k(t)}} - 1} - H(\mathbf{p}_k(t), w_k(t)) \right\} \right\} = \eta_0
\end{aligned} \tag{42}$$

- 
- [26] X. Pei, H. Yu, X. Wang, Y. Chen, M. Wen, and Y. Wu, "NOMA-based Pervasive Edge Computing: Secure Power Allocation for IoV," *IEEE Transactions on Industrial Informatics*, Jun. 2020.
  - [27] D. Liu, M. Zhao, and W. Zhou, "Optimal Offloading Strategy in NOMA-Assisted Mobile Edge Computing," in *International Conference on Wireless Communications and Signal Processing (WCSP)*, Xi'an, China, 2019, pp. 1–6.
  - [28] Z. Ning, X. Wang, and J. Huang, "Mobile Edge Computing-Enabled 5G Vehicular Networks: Toward the Integration of Communication and Computing," *IEEE Vehicular Technology Magazine*, vol. 14, no. 1, pp. 54–61, Mar. 2019.
  - [29] Z. Ning, X. Wang, J. J. P. C. Rodrigues, and F. Xia, "Joint Computation Offloading, Power Allocation, and Channel Assignment for 5G-Enabled Traffic Management Systems," *IEEE Transactions on Industrial Informatics*, vol. 15, no. 5, pp. 3058–3067, May 2019.
  - [30] Z. Wei and H. Jiang, "Optimal Offloading in Fog Computing Systems With Non-Orthogonal Multiple Access," *IEEE Access*, vol. 6, pp. 49767–49778, Sep. 2018.
  - [31] Q. Wang, L. T. Tan, R. Q. Hu, and Y. Qian, "Hierarchical Energy Efficient Mobile Edge Computing in IoT Networks," *IEEE Internet of Things Journal*, Jun. 2020.
  - [32] L. Qian, Y. Wu, F. Jiang, N. Yu, W. Lu, and B. Lin, "NOMA assisted Multi-task Multi-access Mobile Edge Computing via Deep Reinforcement Learning for Industrial Internet of Things," *IEEE Transactions on Industrial Informatics*, early access, Jun. 2020, doi: 10.1109/TII.2020.3001355.
  - [33] D. Jia, K. Lu, and J. Wang, "A Disturbance-Adaptive Design for VANET-Enabled Vehicle Platoon," *IEEE Transactions on Vehicular Technology*, vol. 63, no. 2, pp. 527–539, Feb. 2014.
  - [34] M. Treiber and A. Hennecke, "Congested Traffic States in Empirical Observations and Microscopic Simulations," *Physical review E*, vol. 62, no. 2, pp. 1805–1824, Aug. 2000.
  - [35] Y. Chen, M. Wen, L. Wang, W. Liu, and L. Hanzo, "SINR-Outage Minimization of Robust Beamforming for the Non-Orthogonal Wireless Downlink," *IEEE Transactions on Communications*, vol. 68, no. 11, pp. 7247–7257, Nov. 2020.
  - [36] Y. Mao, C. You, J. Zhang, K. Huang, and K. B. Letaief, "A Survey on Mobile Edge Computing: The Communication Perspective," *IEEE Communications Surveys & Tutorials*, vol. 19, no. 4, pp. 2322–2358, 4th Quart., 2017.
  - [37] C. You, K. Huang, H. Chae, and B. Kim, "Energy-Efficient Resource Allocation for Mobile-Edge Computation Offloading," *IEEE Transactions on Wireless Communications*, vol. 16, no. 3, pp. 1397–1411, Mar. 2017.
  - [38] M. Grant, S. Boyd (2020). *CVX: MATLAB Software for Disciplined Convex Programming*. [Online]. Available: <http://cvxr.com/cvx/>.